



HAL
open science

Probing the path-length dependence of parton energy loss via scaling properties in heavy ion collisions

François Arleo, Guillaume Falmagne

► To cite this version:

François Arleo, Guillaume Falmagne. Probing the path-length dependence of parton energy loss via scaling properties in heavy ion collisions. *Physical Review D*, 2024, 109 (5), pp.L051503. 10.1103/PhysRevD.109.L051503 . hal-03908170

HAL Id: hal-03908170

<https://hal.science/hal-03908170v1>

Submitted on 16 Jan 2025

HAL is a multi-disciplinary open access archive for the deposit and dissemination of scientific research documents, whether they are published or not. The documents may come from teaching and research institutions in France or abroad, or from public or private research centers.

L'archive ouverte pluridisciplinaire **HAL**, est destinée au dépôt et à la diffusion de documents scientifiques de niveau recherche, publiés ou non, émanant des établissements d'enseignement et de recherche français ou étrangers, des laboratoires publics ou privés.



Distributed under a Creative Commons Attribution 4.0 International License

Probing the path-length dependence of parton energy loss via scaling properties in heavy ion collisions

François Arleo¹ and Guillaume Falmagne^{1,2,3}

¹*SUBATECH UMR 6457 (IMT Atlantique, Université de Nantes, IN2P3/CNRS),
4 rue Alfred Kastler, 44307 Nantes, France*

²*Laboratoire Leprince-Ringuet, CNRS/IN2P3, École polytechnique,
Institut Polytechnique de Paris, Palaiseau, France*

³*High Meadows Environmental Institute, Guyot Hall, Princeton University,
Princeton, New Jersey 08544-1003, USA*



(Received 6 December 2022; revised 27 June 2023; accepted 20 February 2024; published 20 March 2024)

The scaling property of large- p_{\perp} hadron suppression, $R_{AA}(p_{\perp})$, measured in heavy ion collisions at the relativistic heavy ion collider and at the large hadron collider (LHC) leads to the determination of the average parton energy loss $\langle \epsilon \rangle$ in quark-gluon plasma produced in a variety of collision systems and centrality classes. Relating $\langle \epsilon \rangle$ to the particle multiplicity and collision geometry allows for probing the dependence of parton energy loss on the path length L . We find that $\langle \epsilon \rangle \propto L^{\beta}$ with $\beta = 1.02_{-0.06}^{+0.09}$, which is consistent with the perturbative quantum chromodynamics expectation of parton energy loss in a longitudinally expanding quark-gluon plasma. We then demonstrate that the azimuthal anisotropy coefficient divided by the collision eccentricity, v_2/e , follows the same scaling property as R_{AA} . This scaling is observed in data, which are reproduced by the model at large p_{\perp} . Finally, a linear relationship between v_2/e and the logarithmic derivative of R_{AA} is found and confirmed in data, offering an additional way to probe the L dependence of parton energy loss using coming measurements from LHC run 3.

DOI: [10.1103/PhysRevD.109.L051503](https://doi.org/10.1103/PhysRevD.109.L051503)

The theory of parton energy loss in quark-gluon plasma (QGP) and its associate jet quenching phenomenology in heavy ion collisions have become increasingly mature over the past decade, triggered by the measurements at the relativistic heavy ion collider (RHIC) and at the large hadron collider (LHC) measurements with unprecedented precision and variety. While in the 2000s the attention had been put on the quenching of single hadron spectra and di-hadron correlations, the focus has then naturally shifted towards jet observables, as a result of new experimental measurements and theoretical ideas (see Refs. [1,2] for recent reviews). Although related in principle, high- p_{\perp} hadrons and jets are likely to probe different aspects of medium-induced gluon radiation. The former appears as a good proxy of genuine parton energy loss in QGP, as originally designed in the theoretical formalisms [3–10]; the latter, instead, probes the gluon emission off a final state made of multiple particles acting coherently [11]. Despite these advances, fundamental questions remain. Among them, how parton energy loss in QGP depends

parametrically on the medium path length L —addressed in many studies [12–19]—is discussed here.

We pursue in this article the approach initiated in Ref. [20], aiming at the understanding of large- p_{\perp} hadron production in heavy ion collisions within a data-driven strategy based on a simple analytic energy loss model. Similar studies have been performed in Refs. [21–24] on jet quenching. Despite obvious limitations, this philosophy may reveal physical properties in data such as scaling laws. This was the case in Ref. [20] where R_{AA} is shown to be a universal function of $p_{\perp}/\bar{\epsilon}$, with $\bar{\epsilon}$ being a characteristic energy loss scale in a given collision system. Starting from this result, confirmed presently using additional datasets, we first explore the relation between $\bar{\epsilon}$ and the multiplicity density n_0 , $\bar{\epsilon} \propto n_0 L^{\beta}$, eventually allowing us to extract the parametric path-length dependence of parton energy loss in QGP. We then use this dependence to determine the azimuthal anisotropy coefficient divided by the collision eccentricity, v_2/e . This ratio follows the same scaling property as R_{AA} , as confirmed in data. Finally, a simple relation between v_2/e and R_{AA} is found, offering a novel and data-driven way to probe the path-length dependence of parton energy loss.

As detailed in Ref. [20], the nuclear modification factor of hadrons at large p_{\perp} is given in the analytic energy loss model by

Published by the American Physical Society under the terms of the [Creative Commons Attribution 4.0 International license](https://creativecommons.org/licenses/by/4.0/). Further distribution of this work must maintain attribution to the author(s) and the published article's title, journal citation, and DOI. Funded by SCOAP³.

TABLE I. R_{AA} data used in this article. The D and J/ψ meson data are used only in Fig. 1.

Species	Collision	\sqrt{s} [TeV]	n	Experiment
π^0	AuAu	0.2	7.7	PHENIX [29]
h^\pm	PbPb	2.76	5.5	ALICE [30], ATLAS [31], CMS [32]
h^\pm	PbPb	5.02	5.5	ALICE [30], CMS [33]
h^\pm	XeXe	5.44	5.3	CMS [34]
D	PbPb	5.02	5.3	ALICE [35], CMS [36]
J/ψ	PbPb	5.02	5.9	ATLAS [37], CMS [38]

$$R_{AA}^h(p_\perp) = \int_0^\infty d\epsilon P(\epsilon) \frac{d\sigma_{pp}^h(p_\perp + \langle z \rangle \epsilon)}{dy dp_\perp} \bigg/ \frac{d\sigma_{pp}^h(p_\perp)}{dy dp_\perp}, \quad (1)$$

where $\langle z \rangle$ is the average momentum fraction carried away by the hadron, which we take independent of p_\perp at LHC based on next-to-leading order calculations [25]. The quenching weight $P(\epsilon)$ is the probability distribution in the energy loss incurred by the parent parton (which we assume for now to be a gluon) while crossing QGP. At large p_\perp , hadron spectra in pp collisions exhibit an almost perfect power law behavior, $d\sigma_{pp}^h/dp_\perp \propto p_\perp^{-n}$, characterized by a spectral index $n = n^h(\sqrt{s})$ obtained from fits to data, whose values are given in Table I [26]. Using (1), R_{AA}^h thus becomes a scaling function of $p_\perp/\bar{\epsilon}$,

$$R_{AA}^h(p_\perp, \bar{\epsilon}, n) = f(u \equiv p_\perp/\bar{\epsilon}, n), \quad (2)$$

with $\bar{\epsilon} = \langle z \rangle \langle \epsilon \rangle$ and f given by

$$f(u, n) = \int_0^\infty dx \bar{P}(x) \left(1 + \frac{x}{u}\right)^{-n} \quad (3)$$

$$\simeq \int_0^\infty dx \bar{P}(x) \exp\left(-\frac{nx}{u}\right). \quad (4)$$

The rescaled quenching weight, $\bar{P}(x = \epsilon/\langle \epsilon \rangle) \equiv \langle \epsilon \rangle P(\epsilon)$, is computed in [27,28] from the Baier-Dokshitzer-Mueller-Peigné-Schiff (BDMPS) medium-induced gluon spectrum [3,4]. The scaling behavior (2) can be observed at a given collision energy, while the approximate scaling in $p_\perp/n\bar{\epsilon}$, Eq. (4), allows for comparing R_{AA} for different hadron species and collision energies. The *shape* f of R_{AA} as a function of p_\perp is thus fully predicted (once n is fixed). In this data-driven approach, the scales $\bar{\epsilon}$ are left as free parameters obtained by adjusting (3) to R_{AA} data for each collision system [note that although $\bar{\epsilon}$ is proportional to the average parton energy loss, the convolution with the quenching weight is actually performed in Eq. (1)].

With respect to Ref. [20], more systems (XeXe at $\sqrt{s} = 5.44$ TeV, AuAu at $\sqrt{s} = 200$ GeV) and additional R_{AA} measurements of h^\pm , J/ψ and D mesons have been

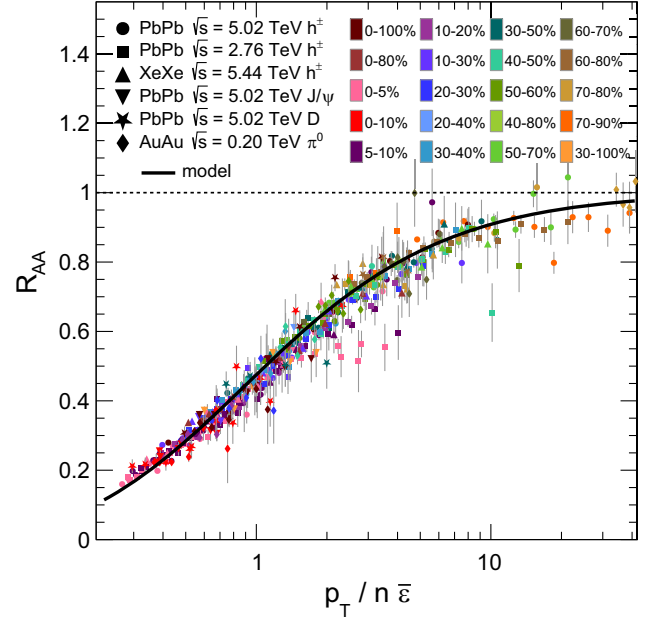


FIG. 1. Scaling of R_{AA} of light hadrons (h^\pm and π^0), D and J/ψ as a function of $p_\perp/n\bar{\epsilon}$, in various collision systems.

included. The selection and geometric bias affecting R_{AA} in a given centrality class is taken into account through a correction factor [39], which does not exceed 4% for centralities below 50%. All the measurements (listed in Table I) with a $p_\perp \gtrsim 10$ GeV cut are plotted in Fig. 1 as a function of $p_\perp/n\bar{\epsilon}$ [40], where $\bar{\epsilon}$ is fitted from R_{AA} in each collision system (i.e., nuclei species, collision energy, and centrality class). Clearly, R_{AA} data line up as predicted into a single universal curve consistent with the shape of R_{AA} given by (2), shown as a solid line. This is consistent with a unique process being responsible for the nuclear modification factors of all hadrons above a given p_\perp .

Our goal is now to relate $\bar{\epsilon}$ extracted from light-hadron data to the relevant physical quantities in heavy ion collisions. In the BDMPS formalism, the average parton energy loss in QGP can be written as [3,4]

$$\langle \epsilon \rangle = \frac{1}{4} \alpha_s C_k \langle \hat{q} \rangle L^2, \quad (5)$$

where L is the average medium path length and C_k is the color charge of the parton ($C_q = 4/3$, $C_g = 3$). The gluon transport coefficient $\langle \hat{q} \rangle$ is linearly averaged along the parton trajectory [41],

$$\langle \hat{q} \rangle = \frac{2}{L^2} \int_{\tau_0}^{\tau_0+L} d\tau (\tau - \tau_0) \hat{q}(\tau), \quad (6)$$

taking into account the dynamical expansion of the medium produced at time τ_0 . The rescaling of the transport coefficient, Eq. (6), should be appropriate for observables sensitive to the primary gluon emission [42,43], which is

the case for the suppression of large- p_\perp hadrons which we address here. The transport coefficient being proportional to the decreasing medium parton density, its time evolution can be parametrized as $\hat{q}(\tau) = \hat{q}_0(\tau_0/\tau)^\alpha$, leading to

$$\langle \hat{q} \rangle = \frac{2}{2-\alpha} \hat{q}_0 \left(\frac{\tau_0}{L} \right)^\alpha \quad (7)$$

for $L \gg \tau_0$. The initial transport coefficient $\hat{q}_0 = \hat{q}(\tau_0)$ and parton density n_0 are directly related, $\hat{q}_0 = (9\pi/2)\alpha_s^2 n_0$ [44]. In the Bjorken picture, n_0 can be estimated as [45]

$$n_0 = \frac{1}{A_\perp \tau_0} \left. \frac{dN_k}{dy} \right|_{y=0} = \frac{3}{2} \frac{1}{A_\perp \tau_0} \left. \frac{dN_{\text{ch}}}{dy} \right|_{y=0}, \quad (8)$$

where A_\perp is the transverse overlap area of the two crossing nuclei. The rightmost equality assumes local parton-hadron duality ($N_k = N_h$) and the factor $N_h/N_{\text{ch}} = 3/2$ takes into account that a third of the produced particles (mostly pions) are electrically neutral. Putting these all together leads to [44]

$$\bar{\epsilon} = K \times \left(\frac{1}{A_\perp} \frac{dN_{\text{ch}}}{dy} L^\beta \right), \quad (9)$$

with $\beta = 2 - \alpha$ and $K = 27\pi/(8\beta) \times \alpha_s^3 \tau_0^{1-\beta} \langle z \rangle_k C_k$.

In the following, we check that the scaling relation Eq. (9) indeed holds for light hadrons in all collision systems. Note that unlike Fig. 1, heavy meson data have not been included in Fig. 2 since their values of $\langle z \rangle_k C_k$ (entering the above expression of K) are likely to differ from that of light hadrons.

The geometric quantities A_\perp and L entering Eq. (9) are determined through an optical Glauber model, assuming hard sphere nuclear densities. The average path length in the transverse plane is given by [46]

$$L \equiv 2 \int d\boldsymbol{\ell} d\mathbf{x} \rho_{\text{coll}}(\mathbf{x}) \rho_{\text{part}}(\mathbf{x} + \boldsymbol{\ell}) |\boldsymbol{\ell}| \quad (10)$$

$$\left/ \int d\boldsymbol{\ell} d\mathbf{x} \rho_{\text{coll}}(\mathbf{x}) \rho_{\text{part}}(\mathbf{x} + \boldsymbol{\ell}), \right.$$

where ρ_{part} and ρ_{coll} are the transverse distributions in the number of participants and of binary nucleon-nucleon collisions, respectively, the latter being the distribution of hard parton production points. The charged particle multiplicity $dN_{\text{ch}}/d\eta$ at midrapidity is taken from PHENIX measurements [47] at RHIC and from ALICE [48–50] and CMS [51,52] measurements at LHC, multiplied by $J = d\eta/dy = 1.25$ at RHIC [53], and $J = 1.09$ at LHC [54].

The energy loss scales $\bar{\epsilon}$ extracted from the quenching of light hadrons are fitted using Eq. (9), with K and β taken as free parameters. Figure 2 exhibits the excellent agreement ($\chi^2/\text{ndf} = 0.51$) obtained with a linear dependence of $\bar{\epsilon}$ with the scaling variable $dN_{\text{ch}}/dy \times L^\beta/A_\perp$. The fits leads to $K = 0.33_{-0.03}^{+0.11} \text{ fm}^{1-\beta}$ and $\beta = 1.02_{-0.06}^{+0.09}$. The uncertainties originate from the fit and from the use of alternative

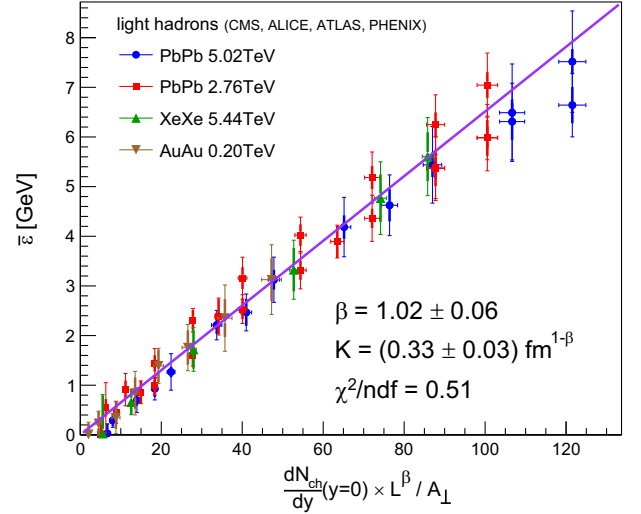


FIG. 2. Average parton energy loss extracted from R_{AA} of light hadrons in various collision systems as a function of $dN_{\text{ch}}/dy \times L^\beta/A_\perp$.

Glauber models for the calculation of L and A_\perp : using constant ρ_{part} , Woods-Saxons nuclear densities, or taken from a Glauber Monte Carlo model [46].

The value of β proves compatible with unity, that is the BDMPS expectation in QGP experiencing a purely longitudinal expansion (i.e. $\alpha = 1$). In particular, it seems to exclude $\langle \epsilon \rangle \propto L^{3-\alpha}$ expected at strong coupling [14,15], at least with reasonable values of α . It is interesting to note that a slightly different path-length dependence of jet energy loss, $\Delta E \propto L^{0.59}$, is obtained in the data-driven approach of Ref. [24]. This is not contradictory: since the final states—large- p_\perp hadrons vs jets—differ in these two studies, there is *a priori* no reason why these should exhibit the same parametric path-length dependence. Similar conclusions apply to the energy dependence, which is at most logarithmic for parton energy loss while an empirical jet energy loss, $\Delta E \propto p_\perp^{0.13}$, is extracted in [24]. This dependence is likely to come from the gluon multiplicity inside a jet which is an increasing function of energy [43].

Turning to the parameter K , its theoretical expectation depends on several uncertain quantities, e.g., the value of α_s ($K \propto \alpha_s^3$), the nature of the propagating parton (hence its color charge), and the fragmentation variable. This being said, the fitted value has the expected magnitude: using $\beta = 1$ (thus making the value of τ_0 irrelevant), $\alpha_s = 0.3$, and $C_g = 3$ for a fragmenting gluon with $\langle z \rangle_g = 0.5$ [25] leads to $K_{\text{th}} = 0.43$.

Although we have assumed so far that only one parton flavor (gluon) fragments into hadrons, contributions from both quark and gluon fragmentation, with respective fraction x_q and $1 - x_q$, should in principle be taken into account. Introducing both flavors leads to an explicit scaling violation in R_{AA} , since x_q is a function of p_\perp but is independent of $\bar{\epsilon}$. We checked, however, that the

scaling behaviors, Eqs. (4) and (9), hold within 2% accuracy in a two-flavor model with a realistic estimate for $x_q(p_\perp)$ [25] and different spectral indices ($n_q \neq n_g$) or fragmentation variables ($\langle z \rangle_q \neq \langle z \rangle_g$) for quarks and gluons. The only sizeable consequence would be a change of K by 15% (that is understood as coming from a weighted average of the color factors C_A and C_F) which is small compared to its theoretical uncertainty [55].

Equation (9) can also be used to predict R_{AA} in other collision systems, such as OO collisions at $\sqrt{s} = 7$ TeV planned at LHC run 3 [56]. Using the nominal Glauber model and the multiplicity from EPOS3.402 [57] gives $\bar{e}_{OO} = 0.61_{-0.10}^{+0.17}$ GeV, leading to $R_{OO}(p_\perp = 20 \text{ GeV}) = 0.85_{-0.02}^{+0.04}$ in minimum bias collisions.

Once the dependence of \bar{e} with L is empirically determined, it becomes possible to investigate the azimuthal dependence of hadron suppression, from which the v_2 coefficient can be computed. Using (2) and (9), the ϕ dependence of R_{AA} can be modeled as

$$R_{AA}(u, n, \phi) = f(u \times (L/L(\phi))^\beta, n), \quad (11)$$

where $L(\phi)$ is given by (10) without the integration on ϕ and with \mathcal{L} along ϕ and $\phi = 0$ is the direction of the impact parameter \mathbf{b} . Let us assume that $L(\phi)$ can be approximated as

$$L(\phi) = L \times (1 - e \cos(2\phi)), \quad (12)$$

where the eccentricity e is thus given by [58]

$$e = \frac{L(\pi/2) - L(0)}{L(\pi/2) + L(0)}. \quad (13)$$

From the definition of the v_m coefficients, we have

$$\frac{R_{AA}(u, n, \phi)}{R_{AA}(u, n)} = 1 + 2 \sum_{m=1}^{\infty} v_{2m} \cos(2m\phi) \quad (14)$$

$$\simeq 1 + 2v_2 \cos(2\phi), \quad (15)$$

where in (15) the higher order harmonics are neglected at high p_\perp [59]. From (11), (12), and (15), one gets

$$\begin{aligned} 2v_2 &\simeq \frac{R_{AA}(0) - R_{AA}(\pi/2)}{R_{AA}(0) + R_{AA}(\pi/2)} \\ &\simeq \frac{f(u/(1-e)^\beta) - f(u/(1+e)^\beta)}{f(u/(1-e)^\beta) + f(u/(1+e)^\beta)}. \end{aligned} \quad (16)$$

Performing the Taylor expansion of (16) to first order in e leads to

$$\frac{v_2(u, n)}{e} \simeq \frac{\beta}{2} \frac{\partial \ln f(u, n)}{\partial \ln u}, \quad (17)$$

$$\frac{v_2(p_\perp)}{e} \simeq \frac{\beta}{2} \frac{p_\perp}{R_{AA}(p_\perp)} \frac{\partial R_{AA}(p_\perp)}{\partial p_\perp}. \quad (18)$$

Within the above assumptions, the quantity v_2/e at large p_\perp is simply proportional to the logarithmic derivative of R_{AA} and to the exponent β . As a consequence, v_2/e has the same universal dependence on p_\perp/\bar{e} as R_{AA} , for all collision energies and centrality classes. It is given by

$$\frac{v_2(u, n)}{e} = \frac{\beta n}{2u} \int dx \bar{P}(x) \frac{x}{(1+x/u)^{n+1}} \bigg/ \int dx \bar{P}(x) \frac{1}{(1+x/u)^n}, \quad (19)$$

using (2) in (17). Equation (18) moreover indicates that v_2 and R_{AA} at a given p_\perp are trivially related for measurements from the same collision system. In particular, this relation does not involve the knowledge of the energy loss scale \bar{e} . Finally, the normalization uncertainties of R_{AA} vanish when computing (18).

In each collision system, a full computation of $R_{AA}(p_\perp, \phi)$ has been performed starting from (11) and using the nominal Glauber model, without any assumption on $L(\phi)$. Fitting $R_{AA}(p_\perp, \phi)$ with (14), restricted to the first three even harmonics, provides an “exact” coefficient v_2 within the model. We find that v_2/e (where e is computed in the Glauber model) is very well reproduced by the approximation (19), plotted in Fig. 3 (gray band), especially for centralities within 5%–60%. It is maximal at low $p_\perp/n\bar{e}$, and smoothly decreases and vanishes in the large- $p_\perp/n\bar{e}$ limit when energy loss effects become negligible. The CMS measurements of v_2 in PbPb collisions at $\sqrt{s} = 2.76$ TeV and $\sqrt{s} = 5.02$ TeV [59,60], reaching up to $p_\perp \simeq 100$ GeV, are also shown in Fig. 3 for $p_\perp > 15$ GeV as a function of the scaling variable $p_\perp/n\bar{e}$, where

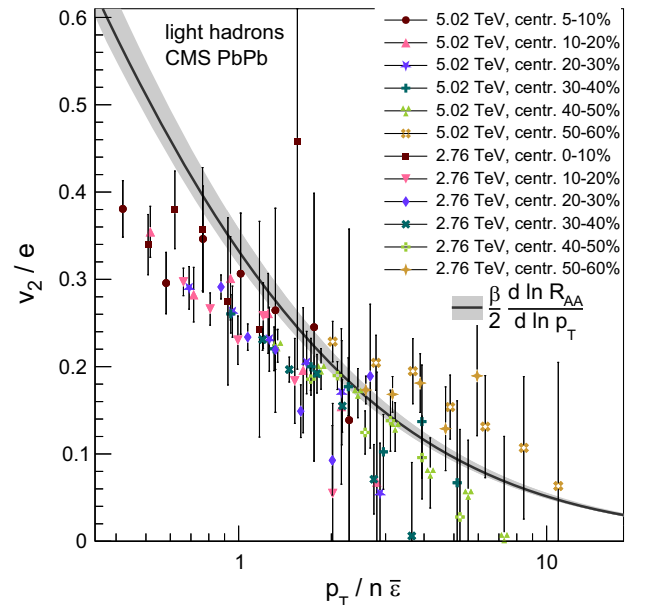


FIG. 3. Scaling of v_2/e of h^\pm in PbPb collisions at $\sqrt{s} = 2.76$ and 5.02 TeV [59,60] as a function of $p_\perp/n\bar{e}$. The solid band $\beta = 1.02_{-0.06}^{+0.09}$ shows Eq. (19) using $n = 5.5$.

the values of \bar{e} originate from the fits of R_{AA} . The predicted scaling for the different collision systems is clearly apparent [61]. Note that the values of \bar{e} are fixed and no longer left as free parameters as in Fig. 1. The model reproduces well the data above $p_{\perp}/n\bar{e} \gtrsim 1$ but over predicts v_2/e at lower values, possibly for the following reason. As path-length fluctuations are neglected [i.e. $R_{AA}(\langle \ell \rangle)$ is computed instead of $\langle R_{AA}(\ell) \rangle_{\ell}$], the model ignores surface emissions and thus over predicts the R_{AA} slope—hence v_2/e —at low p_{\perp} , where R_{AA} is smallest. These fluctuations might, in principle, also affect the scaling Eq. (9); such effects, however, are marginal as β is close to unity (hence $\langle e \rangle \propto \langle \ell^{\beta} \rangle \simeq \langle \ell \rangle^{\beta}$). The effects of the QGP transverse expansion, which is neglected in the calculation of the average path-length consistently with the result $\alpha \simeq 1$, are also known to reduce the anisotropy of R_{AA} at large p_{\perp} and hence the value of v_2 [64].

Despite these limitations, the analytic model appears able to reproduce both R_{AA} and v_2 measurements, at least above $p_{\perp} \gtrsim 15$ GeV. In other words, it does not face the so-called “ $R_{AA} \otimes v_2$ puzzle” investigated by many groups over the last decade [16,18,65–71] and whose resolution might involve event-by-event fluctuations in the soft sector [18] (such fluctuations are naturally absent here as an optical Glauber model is used). The consistency between R_{AA} and v_2 measurements within the present data-driven approach is thus compelling—moreover with a path-length dependence compatible with perturbative QCD, unlike the conclusions of Ref. [16] based on RHIC data. Following the model of Ref. [64], we have also checked that the values of v_2 are reduced by 10%–15% (respectively 20%–30%) for a fluid transverse velocity of $v_{\perp} = 0.1$ (respectively $v_{\perp} = 0.2$), leading to a slightly improved description of the data. This range of values of v_{\perp} is expected in the first few fm/c of the collision [72] while the parton is escaping quark-gluon plasma. Deviations of less than 5% in the scaling behavior of v_2 are expected in the model when including transverse expansion.

While the agreement between the full calculation of v_2/e and Eq. (18) already suggests that this latter relation may be valid, we would like to check whether it also holds when comparing solely R_{AA} and v_2 measurements, independently of the present energy loss model. In order to reduce the uncertainty due to bin-to-bin statistical fluctuations, we perform an agnostic fit (using Chebyshev polynomials) of the CMS R_{AA} data at $\sqrt{s} = 2.76$ TeV and 5.02 TeV [32,33], from which the slope $d \ln R_{AA}/d \ln p_{\perp}$ is evaluated. The v_2/e measurements are plotted as a function of the R_{AA} slope in Fig. 4. Although the present precision of the data does not allow yet for a rigorous test of Eq. (18), the correlation between the two measured quantities is clearly apparent (correlation coefficient $\rho = 0.78$). In addition, the expected function $y = \beta x/2$ (band in Fig. 4) reproduces fairly the observations, giving confidence that the relation between

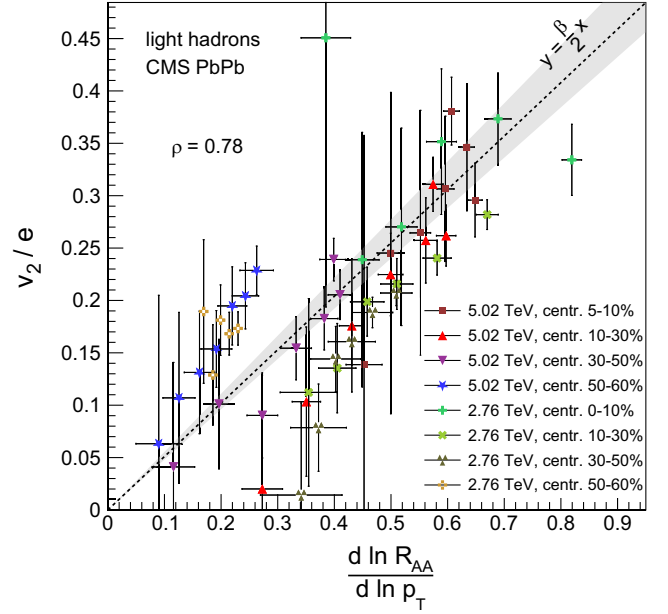


FIG. 4. Relation between v_2/e [59,60] and $d \ln R_{AA}/d \ln p_{\perp}$ [32,33] of h^{\pm} measured by CMS. The band $y = \beta x/2$ ($\beta = 1.02_{-0.06}^{+0.09}$) shows the expectation from (18).

R_{AA} and v_2 at large p_{\perp} gives a direct experimental access to the path-length dependence of parton energy loss in QGP. A slight overshoot in the 50%–60% centrality class v_2 measurements may either signal back-to-back jet correlations contamination in data [33] or the breakdown of (18). In other centrality classes, disagreement may be due to the overestimation of e in the Glauber model nominally used in this work, which relies on hard sphere nuclear densities.

In summary, the universal dependence of hadron R_{AA} at high p_{\perp} has been further checked using additional datasets from RHIC and LHC. Relating the values of \bar{e} extracted from R_{AA} to the hadron multiplicity enables the determination of the L dependence of parton energy loss, $\bar{e} \propto L^{\beta}$ with $\beta = 1.02_{-0.06}^{+0.09}$, in agreement with a longitudinally expanding QGP. The v_2/e anisotropy coefficient exhibits the same scaling property as R_{AA} , in both the model and data. Finally the simple relation between v_2/e and R_{AA} found in the model proved consistent with independent v_2 and R_{AA} measurements, providing another access to the path-length dependence of parton energy loss. The LHC run 3 should allow for testing with unprecedented precision these multiple scaling properties.

We thank Maxime Guilbaud for discussions. G.F. acknowledges the support from IN2P3, and the hospitality of Subatech where this work was completed. This work is funded by the “Agence Nationale de la Recherche” under Grant No. ANR-18-CE31-0024-02, and by a gift from William H. Miller III.

- [1] S. Cao and X.-N. Wang, *Rep. Prog. Phys.* **84**, 024301 (2021).
- [2] L. Cunqueiro and A. M. Sickles, *Prog. Part. Nucl. Phys.* **124**, 103940 (2022).
- [3] R. Baier, Y. L. Dokshitzer, A. H. Mueller, S. Peigné, and D. Schiff, *Nucl. Phys.* **B483**, 291 (1997).
- [4] R. Baier, Y. L. Dokshitzer, A. H. Mueller, S. Peigné, and D. Schiff, *Nucl. Phys.* **B484**, 265 (1997).
- [5] B. G. Zakharov, *JETP Lett.* **63**, 952 (1996).
- [6] B. G. Zakharov, *JETP Lett.* **65**, 615 (1997).
- [7] M. Gyulassy, P. Levai, and I. Vitev, *Nucl. Phys.* **B571**, 197 (2000).
- [8] M. Gyulassy, P. Levai, and I. Vitev, *Nucl. Phys.* **B594**, 371 (2001).
- [9] U. A. Wiedemann, *Nucl. Phys.* **B588**, 303 (2000).
- [10] P. B. Arnold, G. D. Moore, and L. G. Yaffe, *J. High Energy Phys.* **11** (2000) 001.
- [11] J.-P. Blaizot and Y. Mehtar-Tani, *Int. J. Mod. Phys. E* **24**, 1530012 (2015).
- [12] E. V. Shuryak, *Phys. Rev. C* **66**, 027902 (2002).
- [13] S. A. Bass, C. Gale, A. Majumder, C. Nonaka, G.-Y. Qin, T. Renk, and J. Ruppert, *Phys. Rev. C* **79**, 024901 (2009).
- [14] F. Dominguez, C. Marquet, A. H. Mueller, B. Wu, and B.-W. Xiao, *Nucl. Phys.* **A811**, 197 (2008).
- [15] P. M. Chesler, K. Jensen, A. Karch, and L. G. Yaffe, *Phys. Rev. D* **79**, 125015 (2009).
- [16] A. Adare *et al.* (PHENIX Collaboration), *Phys. Rev. Lett.* **105**, 142301 (2010).
- [17] B. Betz and M. Gyulassy, *J. High Energy Phys.* **08** (2014) 090; **10** (2014) 43(E).
- [18] J. Noronha-Hostler, B. Betz, J. Noronha, and M. Gyulassy, *Phys. Rev. Lett.* **116**, 252301 (2016).
- [19] M. Djordjevic, D. Zigic, M. Djordjevic, and J. Auvinen, *Phys. Rev. C* **99**, 061902 (2019).
- [20] F. Arleo, *Phys. Rev. Lett.* **119**, 062302 (2017).
- [21] M. Spousta and B. Cole, *Eur. Phys. J. C* **76**, 50 (2016).
- [22] M. Spousta, *Phys. Lett. B* **767**, 10 (2017).
- [23] Y. He, L.-G. Pang, and X.-N. Wang, *Phys. Rev. Lett.* **122**, 252302 (2019).
- [24] J. Wu, W. Ke, and X.-N. Wang, *Phys. Rev. C* **108**, 034911 (2023).
- [25] R. Sassot, P. Zurita, and M. Stratmann, *Phys. Rev. D* **82**, 074011 (2010).
- [26] Assuming a $\pm 5\%$ variation of the local slope $n(p_{\perp})$ from low to high p_{\perp} leads to negligible scaling violations and does not affect our results.
- [27] R. Baier, Y. L. Dokshitzer, A. H. Mueller, and D. Schiff, *J. High Energy Phys.* **09** (2001) 033.
- [28] F. Arleo, *J. High Energy Phys.* **11** (2002) 044.
- [29] A. Adare *et al.* (PHENIX Collaboration), *Phys. Rev. C* **87**, 034911 (2013).
- [30] S. Acharya *et al.* (ALICE Collaboration), *J. High Energy Phys.* **11** (2018) 013.
- [31] G. Aad *et al.* (ATLAS Collaboration), *J. High Energy Phys.* **09** (2015) 050.
- [32] S. Chatrchyan *et al.* (CMS Collaboration), *Eur. Phys. J. C* **72**, 1945 (2012).
- [33] V. Khachatryan *et al.* (CMS Collaboration), *J. High Energy Phys.* **04** (2017) 039.
- [34] A. M. Sirunyan *et al.* (CMS Collaboration), *J. High Energy Phys.* **10** (2018) 138.
- [35] S. Acharya *et al.* (ALICE Collaboration), *J. High Energy Phys.* **10** (2018) 174.
- [36] A. M. Sirunyan *et al.* (CMS Collaboration), *Phys. Lett. B* **782**, 474 (2018).
- [37] M. Aaboud *et al.* (ATLAS Collaboration), *Eur. Phys. J. C* **78**, 762 (2018).
- [38] A. M. Sirunyan *et al.* (CMS Collaboration), *Eur. Phys. J. C* **78**, 509 (2018).
- [39] C. Loizides and A. Morsch, *Phys. Lett. B* **773**, 408 (2017).
- [40] For clarity, only statistical uncertainties are shown and data points with uncertainties larger than 0.1 are removed.
- [41] C. A. Salgado and U. A. Wiedemann, *Phys. Rev. Lett.* **89**, 092303 (2002).
- [42] S. P. Adhya, C. A. Salgado, M. Spousta, and K. Tywoniuk, *J. High Energy Phys.* **07** (2020) 150.
- [43] P. Caucal, E. Iancu, and G. Soyez, *J. High Energy Phys.* **04** (2021) 209.
- [44] M. Gyulassy, I. Vitev, and X. N. Wang, *Phys. Rev. Lett.* **86**, 2537 (2001).
- [45] J. D. Bjorken, *Phys. Rev. D* **27**, 140 (1983).
- [46] C. Loizides, J. Kamin, and D. d’Enterria, *Phys. Rev. C* **97**, 054910 (2018); **99**, 019901(E) (2019).
- [47] A. Adare *et al.* (PHENIX Collaboration), *Phys. Rev. C* **93**, 024901 (2016).
- [48] J. Adam *et al.* (ALICE Collaboration), *Phys. Rev. Lett.* **116**, 222302 (2016).
- [49] K. Aamodt *et al.* (ALICE Collaboration), *Phys. Rev. Lett.* **106**, 032301 (2011).
- [50] S. Acharya *et al.* (ALICE Collaboration), *Phys. Lett. B* **790**, 35 (2019).
- [51] S. Chatrchyan *et al.* (CMS Collaboration), *J. High Energy Phys.* **08** (2011) 141.
- [52] A. M. Sirunyan *et al.* (CMS Collaboration), *Phys. Lett. B* **799**, 135049 (2019).
- [53] S. S. Adler *et al.* (PHENIX Collaboration), *Phys. Rev. C* **71**, 034908 (2005); **71**, 049901(E) (2005).
- [54] V. Khachatryan *et al.* (CMS Collaboration), *Phys. Rev. Lett.* **105**, 022002 (2010).
- [55] F. Arleo and G. Falmagne (to be published).
- [56] J. Brewer, A. Mazeliauskas, and W. van der Schee, *arXiv*: 2103.01939.
- [57] K. Werner, B. Guiot, I. Karpenko, and T. Pierog, *Phys. Rev. C* **89**, 064903 (2014).
- [58] This definition of e is different than the usual eccentricity $\varepsilon = (\langle y \rangle^2 - \langle x \rangle^2) / (\langle y \rangle^2 + \langle x \rangle^2)$ used to scale v_2 at low p_{\perp} .
- [59] A. M. Sirunyan *et al.* (CMS Collaboration), *Phys. Lett. B* **776**, 195 (2018).
- [60] S. Chatrchyan *et al.* (CMS Collaboration), *Phys. Rev. Lett.* **109**, 022301 (2012).
- [61] The data in the 0%–5% centrality class, not shown here, are subject to important fluctuations [62,63] that also affect the estimation of e . They deviate from the scaling observed in the other classes.
- [62] M. Miller and R. Snellings, *arXiv*:nucl-ex/0312008.
- [63] R. S. Bhalerao and J.-Y. Ollitrault, *Phys. Lett. B* **641**, 260 (2006).

- [64] M. Gyulassy, I. Vitev, X.-N. Wang, and P. Huovinen, *Phys. Lett. B* **526**, 301 (2002).
- [65] D. Molnar and D. Sun, [arXiv:1305.1046](https://arxiv.org/abs/1305.1046).
- [66] J. Xu, A. Buzzatti, and M. Gyulassy, *J. High Energy Phys.* **08** (2014) 063.
- [67] S. K. Das, F. Scardina, S. Plumari, and V. Greco, *Phys. Lett. B* **747**, 260 (2015).
- [68] C. Andres, N. Armesto, H. Niemi, R. Paatelainen, and C. A. Salgado, *Phys. Lett. B* **803**, 135318 (2020).
- [69] D. Zigic, B. Ilic, M. Djordjevic, and M. Djordjevic, *Phys. Rev. C* **101**, 064909 (2020).
- [70] W. Zhao, W. Ke, W. Chen, T. Luo, and X.-N. Wang, *Phys. Rev. Lett.* **128**, 022302 (2022).
- [71] Y. He, W. Chen, T. Luo, S. Cao, L.-G. Pang, and X.-N. Wang, *Phys. Rev. C* **106**, 044904 (2022).
- [72] P. F. Kolb, J. Sollfrank, and U. W. Heinz, *Phys. Rev. C* **62**, 054909 (2000).